Soil pore architecture and irrigation practices in vineyards: evaluation by X-ray micro-tomography

Giacomo Mele[A], Marcella Matrecano[A], José Moràbito[B] and Santa Salatino[B]

[A]Istituto per i Sistemi Agricoli e Forestali del Mediterraneo (ISAFOM), Consiglio Nazionale delle Ricerche (CNR), Ercolano, NA, Italy, Email giacomo.mele@cnr.it
[B]Centro Regional Andino (CRA), Instituto Nacional del Agua (INA), Mendoza, Argentina, Email cra_riego@lanet.com.ar

Abstract
Surface soil samples from three experimental plots subject to three different irrigation practices have been scanned by x-ray micro-tomography and 3D images have been reconstructed and analysed. Pore size distribution and connectivity analysis of the samples showed that drip irrigation with no tillage practice produced the most heterogeneous size range with the highest vertical connectivity of the pore network.

Key Words
X-ray micro-tomography, soil porosity, irrigation, soil image analysis.

Introduction

Soil structure at the pore scale is a key to understanding soil physical, chemical and biological processes (Kutilek and Nielsen 2007; Aochi and Farmer 1995; Young and Ritz 2000). Since the seventies quantification of pore geometry has been achieved by means of image analysis techniques (Jongerius *et al.* 1972, Ismail 1975) on 2D sections of soil blocks impregnated with resin. Walker and Trudgil (1983) have been among the first to point out the need of a three-dimensional representation of the pore space. Such a need has also been demonstrated comparing 2D and 3D images of both natural soil (Moreau *et al*. 1999) and different inhomogeneous virtual pore media (Sevostianov *et al.* 2004). Recent advances in non-destructive 3D imaging systems allow to overcome most of the limitations in image resolution, sample size and time consumption (Cousin *et al.* 1996, Vogel 1997, Mele *et al*. 1999) which for a fairly long time have braked proliferation of 3D soil pore visualisation and quantification. X-ray micro-tomography based on synchrotron radiation or micro-focus cone beam source has become the most applied technique to represent the soil pore architecture at few micron scale, actually enhancing the potential to address soil processes related to real applicative problems (Appoloni *et al.* 2007, Peth *et al.* 2008, Kribaa *et al.* 2001). Pagliai *et al.* 1983, Shiptalo and Protz 1987, Mermut *et al.* 1992, Pagliai *et al.* 2004, Kribaa *et al.* 2001, are examples of studies in which the link between soil pore geometry and agricultural practices has been investigated. In this work we focus on the changes of soil surface structure due to three different irrigation practices under study in a vineyard area in the basin of the Mendoza river (Argentina). 3D image analysis procedures have been used in order to calculate size distribution and connectivity of the pore network of three samples reconstructed by micro focus cone beam X-ray micro-tomography.

Methods

Study site, experimental plots and material

Undisturbed soil samples were collected at the experimental farm of the Instituto National de Tecnologìa Agropecuaria located in Chacras de Coria, department of Luján de Cuyo, Mendoza, Argentina (32º 59’ S, 68º 52’ W, 920.82m a.s.l.). It is an alluvial area in the basin of the Mendoza river where furrow irrigation is largely used in vineyards. Soil shows a silty-loamy texture, a very low organic matter content and is rich in potassium and phosphorus (Romanella 1957). In the experimental vineyard (cv Syrah) three irrigation practices were used: furrow irrigation (LT=labranza traditional), drip irrigation with no tillage (LC=labranza cero) and irrigation by submersion with grass covered surface (CV=cobertura vegetal). Soil samples were collected by aluminium cylinders; in this study three subsurface sample volumes (about 30 cm^3), taken between rows, were examined.

Image reconstruction

The SKYSCAN 1172 desktop micro-tomograph (www.skyscan.be) has been used for the reconstruction of the images. The system is based on a cone microfocus beam source with a tungsten X-ray tube having focal spot of 5 microns (at 4W). Voltage can be set from 20 to 100 kV with current which meets 250 A. The detector is an high resolution CCD camera (4000x2624 pixels) coupled with a FOS (Fiber Optic plate with

X-ray Scintillator) which allows high X-ray sensitivity and wide acquisition area. System has copper and aluminium filter plates which can be used if needed in order to increase the tungsten energy spectrum. Image reconstruction software NRecon (www.skyscan.be) is based on last generation algorithms which apply both "convolution" and "back-projection" procedures. Filtering and correction procedures for "ring artifact" and "beam hardening" (due to the polychromatic source) are included in order to enhance accuracy of the reconstructed images. Rotation of the sample is variously programmable and can be set specifically to avoid artifact due to metal materials in the sample. Resolution of the reconstructed images has been set at 10 microns per voxel; this means that in the following only porosity larger than 10 microns has been considered.

Image analysis
Images have been visualized using the Image ProPlus package (www.mediacy.com). Pore size distribution quantification has been performed using the successive "Opening" algorithm based on procedures of mathematical morphology (Serra 1982, Soille 2003) whose application to the soil porosity have been pointed out by Horgan (1998). Pore connectivity has been measured by propagation methods on the pore network between two opposite edges of an image after steps of opening using the approach described by Lantuejoul and Maisonneuve (1984). These operations allow to draw the "percolation curve" which indicates the percent of the pore space connected, at a given pore diameter, with two opposite sides of a ROI (region of interest) till reaching the throat threshold values for the pore network. Such algorithms have been implemented by the authors in Matlab environment (www.matlab.com).

Results
Solid and pore phase of the three soil samples are shown in Figure 1. Cubic regions of interests (ROIs) having side of 3.5 mm have been visualised and analysed. The results of the pore size distribution and connectivity are shown in Figure. 2 and Figure 3, respectively.

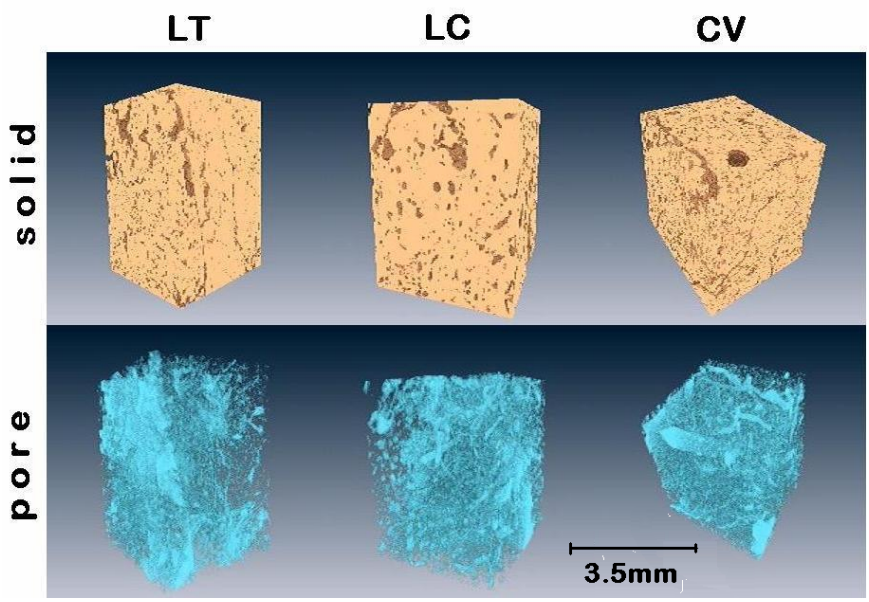

Figure 1. Visualisation of the solid and pore phase of the three samples at 10 micron image resolution. Volumes are cubes with side of 3.5mm.

Differences in porosity values (see the box in Figure 2) highlighted the compactness of the sample from the furrow irrigated plot (LT). This showed also a narrow pore size distribution (Figure 2) around the modal value of 90 microns and a porosity peak around 550 microns due to presence of not continuous cracks (see Figure 1); no continuous paths (larger than image voxel resolution) resulted in the pore network (see LT line in Figure 3). The CV sample (water submersion with grass covered surface) showed an higher and slightly wider pore size distribution around the modal value of 110 microns; porosity peaks around 550 microns and in the range between 1000 and 1300 micron were due to the presence of large tubular pores left by the roots of the grass cover. In the LC case a multi-modal pore size distribution resulted in the range 0-500 microns, indicating the highest heterogeneity of pores in this size range. Complexity of the pore space organisation can be generally considered as a good indicator of soil physical quality due to, for example, the plurality of habitats available for microbiological activity and the better effectiveness of water and air flow for the functioning of the roots.

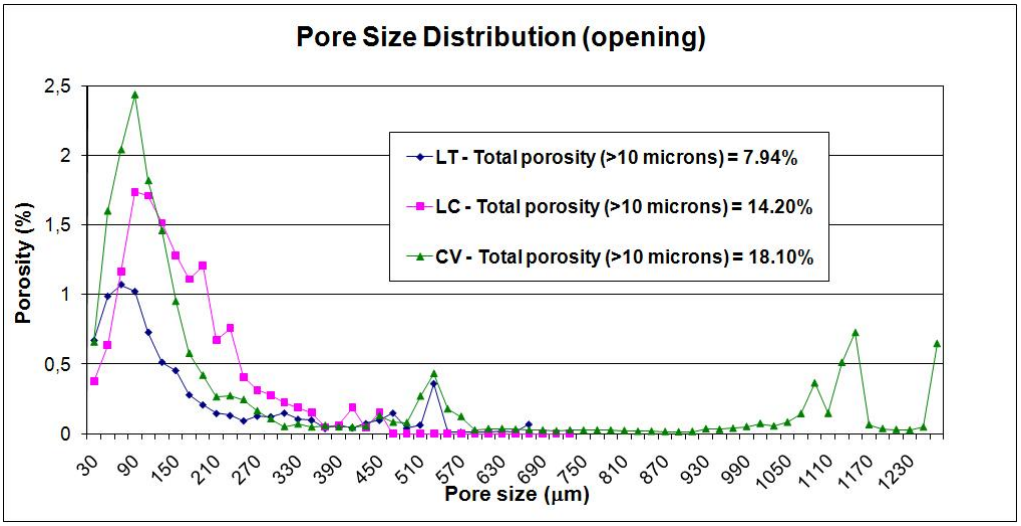

Figure 2. Pore size distribution of the three samples calculated using the "opening" algorithm (Serra 1982, Soille 2003). Porosity having size lower than the image voxel resolution has not been taken into account.

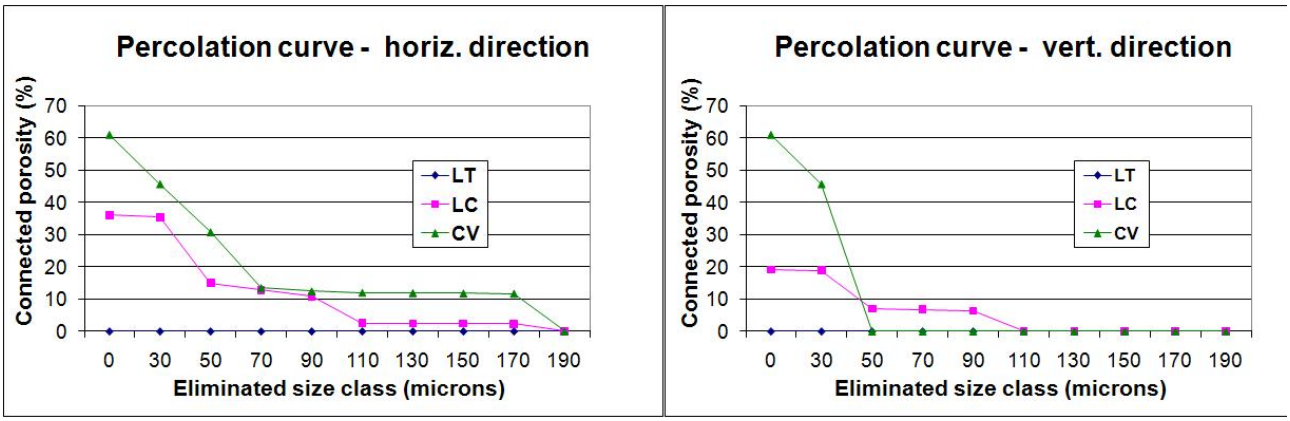

Figure 3. Horizontal and vertical pore connectivity (>10 microns) evaluated by the "percolation curve" procedure (Lantuejoul and Maisonneuve 1984).

Percolation curves (Figure 3) indicated that the pore network of both LC and CV samples were more connected in horizontal than vertical direction. In the LC case 35% and 20% of total porosity resulted to be connected in horizontal and vertical direction, respectively while percolation thresholds were of 190 and 110 microns, respectively. In the CV case 60% of porosity resulted to be connected in both vertical and horizontal direction, but the vertical percolation threshold showed a lower value of 50 microns. Therefore the CV sample, notwithstanding its highest porosity, exhibited narrower necks in vertical direction than in the case of the LC sample, allowing to presume a worse fluid flow in the pore network.

Conclusions

The pore size distribution of the sample of the furrow irrigated plot (LT) showed the lowest presence of pores in the whole size range and allowed to quantify the extreme compactness in soil induced by such irrigation practice. The CV irrigation practice produced the highest value of soil porosity, however the resulting pore size distribution and connectivity analysis indicated a lower soil structure quality than that of the LC case, where total porosity was better distributed in the 0-500 microns pore size range and the highest vertical percolation threshold value was measured.

Results shown in this paper are part of a multi-approach more general investigation to evaluate convenience in changing the traditional irrigation practice in the area of the Mendoza river (Argentina), in order to enhance water use efficiency and crop quality. They overall demonstrate the useful contribution of the 3D pore image analysis in understanding the consequences of the three alternative practices under study on the subsurface soil pore architecture.

Acknowledgements
This work has been carried out in the framework of the scientific cooperation between CNR (Italy) and CONICET (Argentina) "Ecophysiology of irrigated fruit crops: analysis of processes and its application to productivity improvement" (2003-2008).

References

Aochi YO, Farmer WJ (2005) Impact of soil microstructure on the molecular transport dynamics of 1,2-dichloroethane. *Geoderma* **127**, 137-153.

Appoloni CR, Fernandes CP, Rodrigues CRO (2007) X-ray microtomography study of a sandstone reservoir rock. *Nuclear Instruments & Methods in Physics Research*, **80**, 629-632.

Cousin I, Levitz P, Bruand A, (1996) Three-dimensional analysis of a loamy-clay soil using pore and solid chord distributions. *European Journal of Soil Science* **47**, 439–452.

Horgan GW (1998) Mathematical morphology for analysing soil structure from images. *European Journal of Soil Science* **49**, 161-173.

Ismail SNA (1975) Micromorphometric soil porosity characteristics by means of electro-optical image analysis_Quantimet 720., Soil Survey Papers, No. 9. Netherlands Soil Survey Institute, Wageningen

Sevostianov I, Agnihotri G, Garay JF (2004) On connections between 3D microstructures and their 2D images. *International Journal of Fracture* **126**, 65-72.

Jongerius A, Schoonderbeek D, Jager A, Kowalalinski T (1972). Electro-optical soil porosity investigation by means of Quantimet-B equipment *Geoderma* **7**, 177–198

Kribaa M, Hallaire V, Curmi P, Lahmar R (2001) Effect of various cultivation methods on the structure and hydraulic properties of a soil in a semi-arid climate. *Soil and Tillage Research* **60**, 43-53

Kutilek M, Nielsen DR (2007) Interdisciplinarity of hydropedology. *Geoderma* **138**, 252–260.

Lantuejoul C, Maisonneuve F (1984). Geodesic methods in quantitative image analysis. *Pattern Recognit.* **17**, 177–187.

Mele G, Basile A, Leone AP, Moreau E, Terribile F, Velde B (1999) The study of soil structure by coupling serial sections and 3D image analysis. In 'Modelling of transport processes in soils. Int. Workshop of EurAgEng's Field of interest on Soil and Water'. (Eds Feyen, K.Wiyo. Leuven) pp.103-117.

Mermut AR, Grevers MCJ, de Jong E (1992) Evaluation of pores under different management systems by image analysis of clay soils in Saskatchewan, Canada. *Geoderma* **53**, 357–372.

Moreau E, Velde B, Terribile F (1999) Comparison of 2D and 3D images of fractures in a Vertisol *Geoderma* **92**, 55–72.

Pagliai M, La Marca M, Lucamante G (1983) Micromorphometric and micromorphological investigations of a clay soil in viticulture under zero and conventional tillage. *J. Soil Sci.* 391-403

Pagliai M, Vignozzi N, Pellegrini S (2004) Soil structure and the effect of management practices. *Soil Tillage Res.* **79**, 131–143.

Peth S, Horn R, Beckmann F, Donath T, Fischer J, Smucker AJM (2008) Three-Dimensional Quantification of Intra-Aggregate Pore-Space Features using Synchrotron-Radiation-Based Microtomography. *Soil Science Society of America Journal*, **72,** 897-907.

Romanella C (1957) Los suelos de la región del río Mendoza". In 'Boletín de studios geográficos. Volumen IV. Instituto de Geografía. Facultad de Filosofía y Letras'. (Universidad Nacional de Cuyo. Mendoza. Argentina).

Serra J (1982) 'Image analysis and mathematical morphology'. (Academic Press, London).

Shipitalo MJ, Protz R (1987) Comparison of morphology and porosity of a soil under conventional and zero tillage. *Canadian Journal of Soil Science* **67**, 445-456.

Soille P (2003) 'Morphological image analysis—Principles and applications'. (Springer, Berlin, Germany).

Vogel HJ, Weller U, Babel U (1993) Estimating orientation and width of channels and cracks in polished soil blocks, a stereological approach. *Geoderma* **56**, 301–316.

Walker PJC, Trudgil ST (1983) Quantimet image analysis of soil pore geometry: comparison with tracer breakthrough curves. *Earth Processes and Landforms* **8**, 465–472.

Young IM, Ritz K (2000) Tillage, habitat space and function of soil microbes. *Soil & Tillage Research* **53**, 201-213.